Controlled Cellular fusion using optically trapped Plasmonic Nano-Heaters

Azra Bahadori[a], Andreas R. Lund [a], Szabolcs Semsey [a], Lene B. Oddershede[a], Poul M. Bendix[*,a]
[a]Niels Bohr Institute, University of Copenhagen, Blegdamsvej 17, DK-2100 Copenhagen

ABSTRACT

Optically trapped plasmonic nano-heaters are used to mediate efficient and controlled fusion of biological membranes. The fusion method is demonstrated by optically trapping plasmonic nanoparticles located in between vesicle membranes leading to rapid lipid and content mixing. As an interesting application we show how direct control over fusion can be used for studying diffusion of peripheral membrane proteins and their interactions with membranes and for studying protein reactions. Membrane proteins encapsulated in an inert vesicle can be transferred to a vesicle composed of negative lipids by optically induced fusion. Mixing of the two membranes results in a fused vesicle with a high affinity for the protein and we observe immediate membrane tubulation due to the activity of the protein. Fusion of distinct membrane compartments also has applications in small scale chemistry for realizing pico-liter reactions and offers many exciting applications within biology which are discussed here.

Keywords: *membrane fusion, giant unilamellar vesicles, I-BAR, membrane nanotubes, plasmonic heating, gold nanoparticles, optical trapping, cell fusion*

1. INTRODUCTION

Lipid membranes are two dimensional sheets which encapsulate every mammalian cell. Additionally, membranes provide the cell with an intracellular architecture providing a labyrinth of nanoscale tubular and liposomal compartments and larger structures like the nucleus. A number of biological processes are associated with membranes and are mediated by membrane interacting proteins. For instance, membrane sculpting, reshaping and fusion are critical processes for facilitating intracellular transport and cell migration. To achieve fusion the cells employ fusion proteins which can bring membranes into close proximity and subsequently mediate full fusion and hence restructure two apposing membranes into a single membrane [1]. The molecular mechanisms behind biological membrane fusion are being intensively studied [2, 3], but a full understanding of the mechanism of fusion requires an understanding of the biophysical aspects of membrane fusion. Physical parameters like tension and curvature have been shown to play a critical role in fusion [4], whereas the effect of temperature on fusion has received little attention despite the realization of the dramatic effect temperature has on fluid lipid membranes [5, 6]. Additionally, thermally induced local phase transitions in membranes [7, 8] can also simulate the raft like cell membrane environment with domain boundaries separating co-existing domains in cell membranes.

Localized heating effects on membranes has been demonstrated using plasmonic heating generated by optical trapping of gold nanoparticles. Gel phase membranes with a well characterized phase transition temperature have been used as thermal sensors for laser irradiated nanoparticles [9] and the localized heating has also been used for studying the effect of heating on membrane permeation in giant unilamellar vesicles (GUVs) [7, 8]. Also, pulsed lasers have been applied to optically inject cell membrane attached gold nanoparticles into cells [10, 11] or to mediate membrane fusion [12]. Recently, a new application of plasmonic heating was demonstrated by mediating membrane fusion by using gold nanoparticles optically trapped, by a near infrared laser, at the contact zone between two giant unilamellar vesicles (GUVs) [13].

Here we demonstrate how GUVs can be readily fused with consequent lipid and content mixing following fusion. By using optical trapping, we bring a selected GUV into close contact with a target GUV and perform fusion by trapping a

*bendix@nbi.dk; phone +45 35325251

Optical Trapping and Optical Micromanipulation XIII, edited by Kishan Dholakia, Gabriel C. Spalding, Proc. of SPIE
Vol. 9922, 992211 · © 2016 SPIE · CCC code: 0277-786X/16/$18 · doi: 10.1117/12.2237848

d = 80 nm gold nanoparticle at the interface. This realization of selected GUV-GUV fusion allows lipid diffusion and nanoscale reactions to be investigated. A novel application of the technique is presented involving membrane shaping proteins which can be encapsulated in GUVs with a certain membrane composition. Finally, we discuss the potential for extending the technique for GUV-cell fusion as well as for cell-cell fusion which could significantly extend the translational impact of the technique.

2. METHODOLOGY

2.1 Optical trapping and imaging

Confocal imaging was performed on a Leica SP5 confocal microscope into which an optical trap, based on a 1064 nm laser (Spectra Physics J201-BL-106C), was implemented. More information regarding the setup is given in Ref. [14]. Fusion was carried out using P = 200 mW at the focal plane of the microscope and by using a Leica PL APO, NA=1.2, 63X water immersion objective to tightly focus the laser light. The optical trap was stationary, but the trap could be moved relative to the GUVs by translating the sample which was mounted on a piezoelectric stage (PI 731.20, Physik Instrumente, Germany) allowing lateral movements with nanometer precision. A glass bottom open chamber, containing the GUVs and gold nanoparticles, was mounted on the microscope and kept at room temperature during the experiment. The *FAST*-DiO and calcein fluorophores as well as the YFP were excited using a 488 nm argon laser line. A 513 nm argon laser line was used to excite the DiIC18 lipophilic fluorophores and a 594 nm laser line was used to excite TR-DHPE lipophilic dye. The emitted intensities were collected using photomultiplier tubes. To detect the scattered and reflected light from the AuNPs, a 476 nm argon laser line was used in reflection mode.

2.2 Sample preparation

Open chambers with a bottom glass coverslip (thickness of 170 μm, Menzel-Gläser) were cleaned by sonication for 5 minutes in detergent followed by three rounds (5 minutes each) of sonication in water and finally 5 minutes of sonication in ethanol. Coating of the glass with 2 g/L α-casein (from Sigma Aldrich) for 10 min followed by triple wash with 150 mM PBS prevented the GUVs from adhering to the glass. Gold nanoparticles purchased from British Biocell International (BBI) were citrate stabilized and had a mean diameter of 80 nm. The nanoparticle solution was gently vortexed and ~10 μL of the stock solution was added to the chamber using a pipette. GUVs were loaded to the chamber by adding 5 μL GUV stock to the sample containing 100 μL PBS buffer containing 150 mM NaCl. The protein and molecule solutions used in the encapsulation experiments (I-BAR and calcein) were also present outside the GUVs in the GUV stock solution and were diluted 20 times in the extra-vesicular solution when added to the chamber, which allowed visualization of the encapsulated I-BAR or calcein.

2.3 Electroformation of GUVs

Standard electroformation was used to form GUVs using a mixture of DOPC lipids (1,2-dioleoyl-sn-glycero-3-phosphocholine, Avanti polar lipids) and DOPS lipids (1,2-dioleoyl-sn-glycero-3-phosphoserine, Avanti polar lipids). The percentage of DOPS was 20% in all experiments except in Figure 4 where I-BAR domains were encapsulated in GUVs made from zwitterionic DOPC which were fused to a GUV containing 40% DOPS. Also, the GUVs contained 0.5% of the lipophilic tracer *FAST*-DiO (3,3'-dilinoleyloxacarbocyanine perchlorate, Invitrogen). The GUVs were hydrated with a 300 mM sucrose solution.

2.4 Protein encapsulation

I-BAR domains were from the protein ABBA which is a member of the IRSp53-MIM protein family [15]. The I-BAR domain was engineered with an N-terminal HIS-tag and a C-terminal YFP-tag. The I-BAR was extracted in high salt (1M) with glycerol and triton X-100 detergent both of which can influence the formation of GUVs. The detergent was removed by dialysis. To form vesicles under these difficult conditions we used gel assisted hydration [16] which uses simple hydration on a microporous gel without the need of an electric field. To coat the surface with gel we added a solution of 1 mL of 5 g/L polyvinyl alcohol (PVA) solution onto a clean glass slide until full coverage. The glass was tilted to let excess solution run off. The freshly coated slides were then baked at 50° C for 30 min (until the PVA film had dried). We deposited a drop (10 μL) of sucrose solution on the PVA film and sandwiched it between the two slides for 1 min to spread the droplet. Lipids in chloroform were shortly thereafter added on top as described above for

electroformation and placed in vacuum for 1 hour to remove all residues of chloroform. Subsequently, the film was hydrated by adding 300 mM sucrose in MilliQ water in an appropriate O-ring confinement (e.g., d = 16 mm) for 1 hour for empty vesicles. Encapsulation of I-BAR was achieved using a hydrating solution consisting of a solution of 50 % PBS (150 mM) and 50% sucrose (300 mM) (volume percentages) mixed with ~10 μL of protein stock solution such that the final concentration of I-BAR was 1.5 μM. The successful progress of hydration and encapsulation was followed on the microscope. The PVA surface with the hydration solution was gently agitated to detach some vesicles from the PVA surface before harvesting the vesicles with a pipette and transferring them to an eppendorf tube.

2.5 Protein expression

Details on the protein expression are given in Ref. [13].

2.6 Data analysis

All images were analyzed using Matlab (The MathWorks, Inc., Natick, Massachusetts, United States). The temperatures calculated in Figure 1B were plotted using Matlab and calculations were based on Mie's equations [17, 18].

2.7 Membrane heating assay

The membrane melting experiments presented in Figure 1D were carried out as described in Ref. [19] where more details are provided. Briefly, a glass supported gel phase bilayer was prepared from vesicles extruded using 50 nm polycarbonate filters (Avanti Polar Lipids, Mini-extruder). The vesicles were made from the saturated DC15PC lipid and 3 mol% of the lipophilic dye, DiIC18 (Invitrogen). Vesicles were allowed to fuse to a piranha etched glass substrate, at T = 37°C, and subsequently formed a two dimensional lipid bilayer. The sample was thoroughly rinsed with MilliQ water 20 times while the temperature was kept at 45-50°C which is above the melting transition of DC15PC (~33°C). Subsequently, the sample was placed on the microscope stage where the temperature was 28°C. Gold nanoparticles adhered to the bilayer were irradiated and the local heating caused melting of the bilayer in a region where the temperature increased above 33°C, as shown in Figure 1D.

3. RESULTS

3.1 Irradiation of gold nanoparticles generates heat

Metallic nanoparticles produce substantial heat when irradiated by light [20, 21]. Light in the optical and near infrared spectrum couple to the oscillating electrons in the particle, called surface plasmon oscillations, and the absorption reaches a maximum when the light is resonant with the oscillation frequency of the surface plasmons [22]. The corresponding resonance wavelength which interacts optimally with typical gold nanostructures of different sizes and shapes lies in the optical and near infrared regime (500-1000 nm) [23]. Spherical gold nanoparticles are well characterized with regard to optical induced heating [20, 21, 24] and other optical properties and they have been shown to heat substantially when exposed to near infrared light despite the fact that their surface plasmons resonate optimally with optical light ($\lambda \sim 530$ nm). Moreover, spherical gold nanoparticles are well characterized with regard to optical trapping and several particle sizes have been trapped by single beam optical tweezers using near infrared light ($\lambda = 1064$ nm) [25, 26].

Using these attractive properties of gold nanoparticles, we performed optically controlled fusion of membranes. The gold nanoparticles were trapped by a single beam optical trap based on a $\lambda = 1064$ nm laser, as presented schematically in Figure 1A. Irradiation of the trapped nanoparticle produced high particle temperatures as well as substantial heating of the surrounding environment which can be calculated using Mie's equations [17, 18]. In Figure 1B we show two such calculations for the temperature profiles of d = 80 nm and d = 150 nm particles, irradiated at 10 MW/cm^2, which are plotted as a function of distance from the particle.

Experimentally, we characterize the nanoparticles using transmission electron microscopy (TEM) as shown in Figure 1C for d = 80 nm (top panel) and d = 150 nm (bottom panel) gold nanoparticles. When placed in a highly focused laser beam ($\lambda = 1064$ nm) these particles produce substantial heat and are able to locally melt a gel phase membrane as demonstrated in Figure 1D. The gold nanoparticles in Figure 1D are immobilized on a gel phase membrane which is composed of a saturated lipid (DC15PC) and 3 mol% of a membrane dye (DiIC18) and the membrane has a phase transition temperature of $T \approx 33$°C. Local heating from the irradiated nanoparticle generates a phase transition with a

fluid phase near the nanoparticle and a gel phase further away from the nanoparticle where the temperature is still ambient and below the phase transition. The fluid phase is detectable as a circular region due to the lower intensity emitted from the dye when incorporated in the fluid phase. Additionally, the dye has a preference for the more ordered gel phase and can become partially depleted from the fluid phase [19, 27, 28]. The size of the circular region in Figure 1D is larger for the d = 150 nm gold nanoparticle (bottom panel) than for the d = 80 nm gold nanoparticle (top panel) since larger nanoparticles generate significantly more heat at the same laser power [19]. The temperature increase as a function of distance from the nanoparticle is found by using the following relationship between temperature increase and distance, D,

$$\Delta T(D) = \frac{CI}{D} \tag{1}$$

where C is a constant which depends on the thermal conductivity of the environment and the size and material of the particle. I is the intensity of light incident on the nanoparticle and is given in power normalized by area.

3.2 Trapped nanoparticles mediate fusion

The heating generated by optically trapped gold nanoparticles is highly localized as the temperature decays to ca. 50% at a distance from the nanoparticle corresponding to the diameter of the nanoparticle. When using nano-sized particles the heated region is therefore sufficiently localized that they can be used to locally apply strong heating to micrometer sized biological specimens like membrane vesicles or cells without inflicting damage to the whole specimen. Therefore, optical trapping of metallic nanoparticles is an ideal tool to mediate fusion between cell membranes like cell sized GUVs and between living cells.

To achieve fusion between two selected GUVs suspended in an aqueous solution in a microscope chamber it is critical that the GUVs are not adhering too firmly to the glass coverslip and also that the GUVs need to be possible to trap using the optical tweezers. Trapping of lipid vesicles has previously been shown to be possible if the vesicles are loaded with sufficiently high concentration sugar solution like sucrose [29]. A solution containing sucrose has a higher index of refraction than the outside solution which is a requirement for trapping. Also, the outside solution should contain iso-osmolar concentrations of salt to avoid osmotic stress on the membrane. Finally, to follow the fusion process which involves lipid and content mixing the GUVs should be labeled with lipid fluorophores and aqueous fluorophores in their lumen.

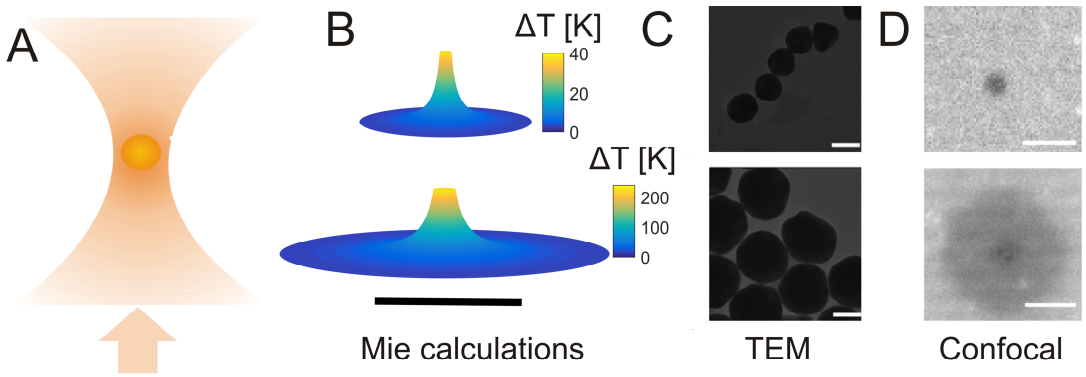

Figure 1 Heating of optically trapped gold nanoparticles. (A) A near infrared (NIR) optical trap is used to confine the gold nanoparticle in 3D. (B) Temperature calculations for two gold nanoparticles (top, d= 80 nm and bottom, d = 150 nm) irradiated by 10MW/cm^2 and λ = 1064 nm. (C) Transmission Electron Micrograph of d = 80 nm (top) and d = 150 nm (bottom) gold nanoparticles purchased from British Biocell International (BBI). Scale bars, 2 µm. (D) Temperature measurements of irradiated d = 80 nm (top) and a d = 150 nm (bottom) gold nanoparticle by using a flat gel phase membrane as a temperature sensor. The local heating generated by the two particles results in melting of a circular area surrounding the nanoparticle which is imaged by using phase sensitive fluorophores (DiIC18). The distance from the nanoparticle to the rim of the signature depends on the nanoparticle temperature. The laser powers used were P = 270 ±5 mW (top) and P = 261 ± 5 mW (bottom). Scale bars, 2 µm.

In Figure 2A we schematically present how a fusion experiment is conducted. First two selected GUVs are brought together into close proximity and subsequently the laser focus is parked at the contact site where the GUVs have a point like contact zone. Finally, after a short waiting time, which depends on the concentration of gold nanoparticles in the sample, a gold nanoparticle will enter the trap and becomes heated which mediates the fusion. This fusion process is shown in Figure 2B where confocal images of the two GUVs are shown. The GUVs are labeled with red and green lipid dyes and upon fusion the two dyes mix by two dimensional diffusion. The intensities from the green and red dyes, as a function of time, are plotted in Figure 2C which reveals that complete mixing is achieved on a time scale of 10 s which is also theoretically predicted by considering mixing of two kinds of lipids initially located in two respective hemispheres [13, 30].

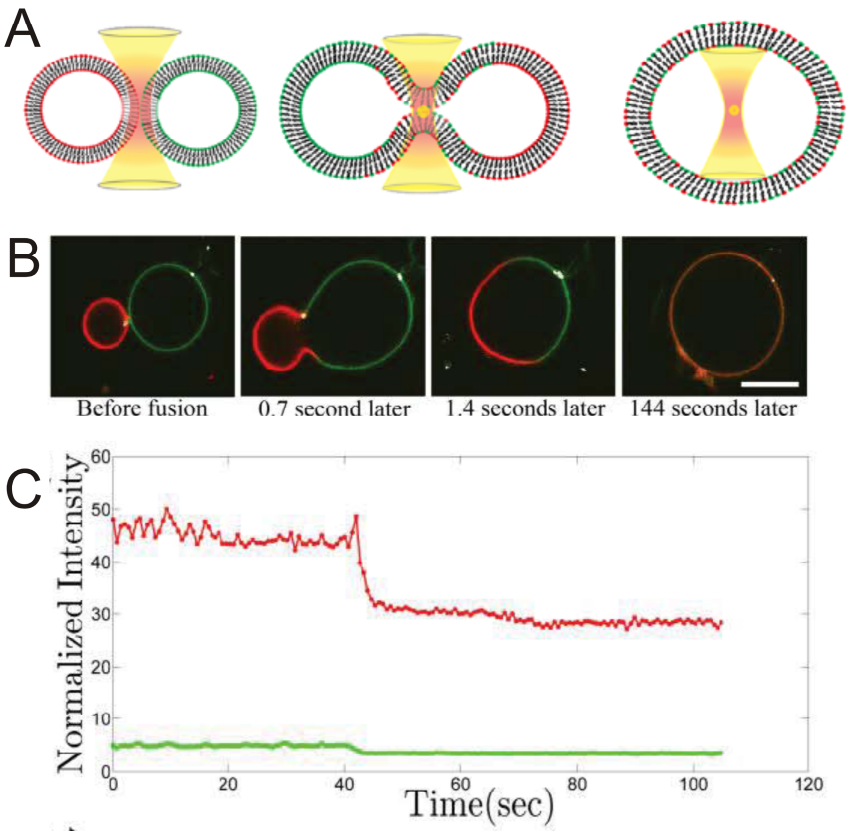

Figure 2 Fusion and subsequent lipid mixing of two GUVs mediated by an optically trapped gold nanoparticle. (A) Schematic presentation of the experiment. Two GUVs labeled with different colored dyes are first selected for fusion and brought together by optical trapping. Optical trapping of a gold nanoparticle at the interface between the GUVs results in full fusion of the two GUVs. (B) Data showing an example of fusion of two GUVs labeled with DiO (green) and TR-DHPE (red), respectively. Fusion is mediated by optical trapping of a *d*= 80 nm gold nanoparticle. (C) Quantification of the intensity of the two GUVs during fusion. Lipid mixing is seen as dilution of the two dyes into a larger area. The time scale of lipid mixing is 1-10 s. The figure is adapted with permission from (Nano Letters 15(6), 4183-4188 (2010)). Copyright (2010) American Chemical Society.

During membrane fusion mixing of the aqueous contents also occurs. The content of one vesicle can be completely delivered to a target vesicle. This is an experiment that has great implications for understanding the mechanism behind drug delivery to cells [31] and it has applications in exploring chemistry in tiny compartments. To visualize the mixing of the compartments of two GUVs, which are selected for fusion, we load one of the GUVs with the aqueous dye calcein as depicted in Figure 3A. By triggering fusion with an optically trapped gold nanoparticle we observe immediate dilution of the calcein dye into the lumen of the fused vesicle as imaged by confocal microscopy in Figure 3B. The diffusion constant of calcein molecules in water has been measured to 333 ± 117 $\mu m^2/s$ [32] which supports the rapid mixing of the two solutions which occurs on a time scale of 1 s, see Figure 3C.

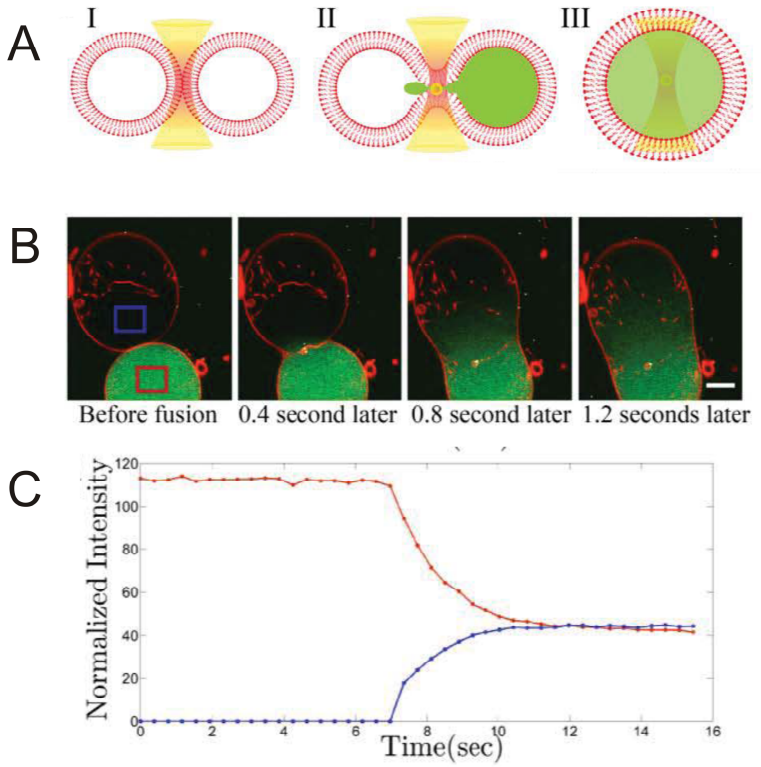

Figure 3 Fusion and content mixing of two GUVs mediated by optical trapping of a gold nanoparticle. (A) Schematic presentation of the experiment showing two GUVs with membranes labeled by a red dye and the lumen of one GUV labeled with a green aqueous dye. Fusion is mediated by positioning the GUVs side by side using an optical trap and subsequently a gold nanoparticle is trapped at the interface between the GUVs to mediated full fusion of the adjacent membranes. (B) Experimental data showing fusion of two GUVs by optical trapping a gold nanoparticle (*d*= 80 nm) at the interface between the GUVs. Upon fusion the calcein in one of the GUVs mixes with the unlabeled lumen of the other GUV. Membranes are labeled using TR-DHPE (red) and the lumen of the lower GUV contains the aqueous dye calcein. (C) Quantification of the lumen intensity inside the blue and red rectangles depicted in the first image in (B). The intensities converge to the same level over a time scale of ~1 s.

The experiments in Figure 2 and Figure 3 demonstrate that GUVs can be fused and also be used for controlling lipid and lumen composition of the fused vesicle. This ability has interesting possibilities in biophysical applications in which protein binding to membranes occurs on the inside of membranes (for example inside cells) and only to negatively charged lipids. The protein domain used in the current study is the I-BAR domain from the ABBA protein which is a convex shaped dimeric membrane protein [33] which transforms flat membranes into tubular structures. The molecular curvature of the domain is imposed on the soft membrane which has implications in cellular structures like filopodia [33,

34] and membrane ruffles [15]. Indeed, when the protein is added to the outside of GUVs we see membrane tubes of uniform diameters protruding into GUVs as shown in Figure 4A [35]. These tubes have been investigated with respect to width and stiffness and were found to have a diameter of ~50 nm and a persistence length of ~4 μm [35].

However, to mimic the cellular settings with the protein binding to a GUV on the inner side of the membrane, the protein needs to be encapsulated inside the GUV. Encapsulation of proteins and molecules has previously been accomplished by simply suspending the protein in the solution which is used to hydrate the lipid film during formation of the GUVs [36]. However, membrane binding proteins will bind to the lipids already during formation of the GUVs and could interfere with the process of vesicle formation.

Optically controlled fusion allows proteins first to be encapsulated inside GUVs composed of zwitterionic lipids (overall neutral charge) and subsequently to be transferred to GUVs containing a fraction of negatively charged lipids which promote binding of the protein as schematically depicted in Figure 4B. Therefore, we first mix the I-BAR with the solution used to hydrate a lipid film consisting of neutral DOPC lipids and trace amounts of membrane dye, FAST-DiO. I-BAR containing GUVs are then optically trapped and located next to GUVs containing 40% DOPS lipids 59% DOPC lipids. Optical trapping of a gold nanoparticle at the contact site between the two GUVs causes mixing of the I-BAR solution into the negatively charged GUV containing DOPS lipids and binding to the membrane causes the membrane to form tubules as shown in Figure 4C [13].

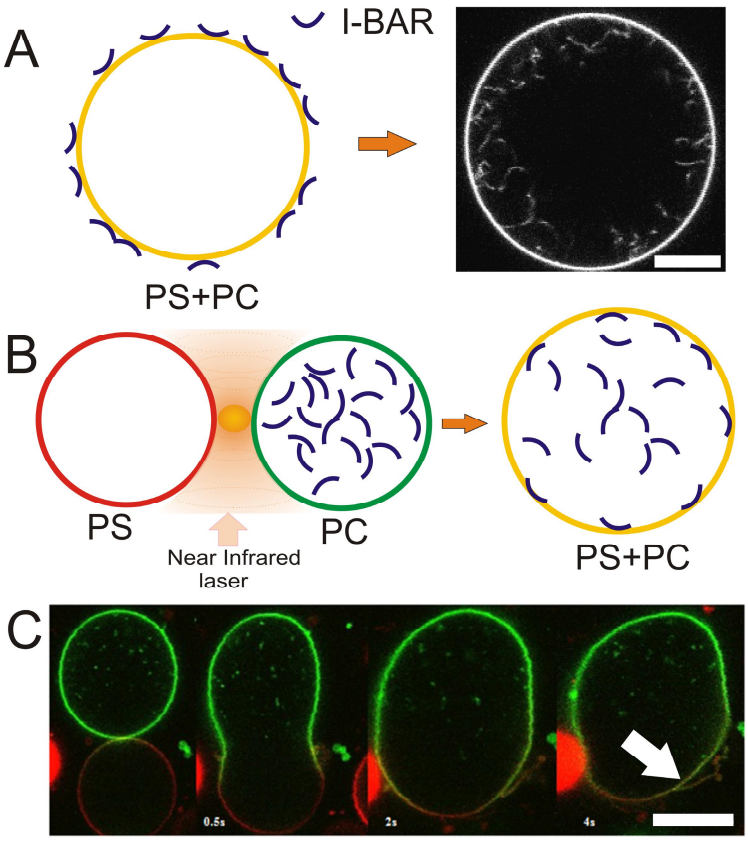

Figure 4 A biophysical application of hot nanoparticle mediated membrane fusion involving membrane shaping by I-BAR domains. (A) I-BAR domains are peripheral membrane binding domains which can bind electrostatically to negatively charged membranes. The right image shows tubular invaginations following exposure of the outer surface of the GUV to I-BARs (2.3 μM). Tubes form due to the convex shape of the protein binding surface. The I-BAR is tagged with yellow fluorescent protein (YFP) which labels both the GUV membrane and the tubular invaginations. (B) Schematic representation of an experiment with I-BARs contained

initially within neutral GUVs and subsequently transferred to GUVs with negatively charged membrane by hot nanoparticle mediated fusion of the two GUVs. Following lipid and lumen mixing the I-BAR binds to the negatively charged surface inside the fused GUV. (C) Experimental data showing fusion between a neutral GUV containing I-BAR with a GUV composed of negatively charged lipids (40% DOPS). After fusion a tubular protrusion is observed in the last image (White arrow). Membranes are labeled with DiO (green) and TR-DHPE (red), respectively. The images in (C) are reused with permission from (Nano Letters 15(6), 4183-4188 (2010)). Copyright (2010) American Chemical Society.

4. DISCUSSION

Optical control of membrane vesicles combined with plasmonic heating provides a useful strategy for manipulating distinct membrane compartments in a highly controlled and selective manner. Individual GUVs are selected in a microscope chamber and readily trapped by a focused laser beam and subsequently positioned next to a target GUV [13]. By having gold nanoparticles suspended in solution with the optical trap turned on and positioned at the contact zone between the GUVs fusion occurs after a certain waiting time which depends on the concentration of nanoparticles in solution.

This technique is particularly promising due to the fact that high temperature increases of 100-200°C, are obtained at the surface of the particle whereas the heated region is extremely localized and only extends a few hundred nanometers away from the nanoparticle surface. Beyond this distance the temperature increase is below ~20°C and continues to decay with distance from the particle. The extent of the heated region can be conveniently tuned by altering the particle size and regulating the laser power. Here, we have focused on the use of d = 80 nm gold nanoparticles which provide significant particle temperatures upon near infrared irradiation (Figure 1B,D, top panels), however, as shown in the bottom panels in Figure 1B,D, larger gold nanoparticles with d = 150 nm can heat substantially larger areas. This offers new and unexplored possibilities to perform fusion with smaller nanoparticles which have a higher photothermal efficiency and hence could mediate fusion with even more localized heating with consequent less biological damage. Increased absorption can be achieved with more absorptive materials or alternatively by designing the particle shape to achieve strong resonance between the surface plasmons in the particle and the infrared light [37-39].

The level of control achieved over membrane fusion makes this technique highly attractive with respect to research in drug delivery to cells if fusion can be carried out between a GUV and the plasma membrane of cells. However, fusion of large vesicles to cells involves transferring large volumes of sucrose solution to cells which could compromise the viability of cells. Therefore, this technique needs to be further developed to allow fusion of smaller vesicles.

Controlled mixing of membrane compartments with diameters of ~10-20 μm allows chemistry to be performed between picoliter volumes while confocal imaging can be used to visualize the mixing of the two lumens with time resolution of ~0.1 s. Faster imaging could also be applied if the imaging modality is compatible with optical trapping. Further development of the technique to allow fusion of ~1 μm vesicles would allow chemistry to be studied at femtoliter volumes.

Biophysically the strategy of fusing GUVs with different membrane compositions opens up a variety of possibilities for exploring lipid mixing, membrane phase behavior and also for investigating membrane interaction with peripheral membrane proteins. Here, we have provided one example where I-BAR proteins were first encapsulated in an inert GUV and subsequently transferred to a GUV where membrane composition allowed electrostatic binding of the protein to the membrane (see Figure 4). The fusion strategy demonstrated here has great potential for studying assembly of cytoskeletal systems like actin filaments in a confined environment. Encapsulation of actin monomers in one GUV and encapsulation of polymerizing factors (ATP, salts etc.) and actin binding proteins (cross-linkers like fascin [40] or α-actinin [41]) in a target GUV allows investigation of actin polymerization and network or bundling formation in real time inside small compartments which have the same dimensions as cells [42].

5. CONCLUSION

Plasmonic heating of optically trapped gold nanoparticles was used to mediate fusion between selected membrane vesicles. Resulting lipid and content mixing was readily monitored by using a confocal microscope in conjunction with the optical trapping. The membranes and lumens of the two respective GUVs were labeled with appropriate fluorophores which allowed us to quantify the mixing time scales of the membranes and lumens. As an application we demonstrate how the technique can be applied in novel biophysical experiments to explore the effect of curvature inducing proteins on membranes. Finally, we note that the current technique contains an undepleted potential for further development with more advanced trapping schemes [43-45] permitting parallel trapping of several biological specimens, including living cells, in conjunction with fluorescent imaging.

ACKNOWLEDGEMENTS

Financial support for the project was received from the Lundbeck Foundation, Center for Biomembranes in Nanomedicine, the Villum Kann Rasmussen Foundation grant number VKR022593, the Danish Council for Independent Research DFF – 4181-00196 and the Danish National Research Foundation grant number DNRF116 and from the Novo Nordisk Foundation (NNF14OC0011361).

REFERENCES

[1] Chen, Y. A. and Scheller, R. H. "Snare-mediated membrane fusion". Nat. Rev. Mol. Cell Biol. 2, 98-106 (2001).
[2] Martens, S. and McMahon, H. T. "Mechanisms of membrane fusion: disparate players and common principles". Nat. Rev. Mol. Cell Biol. 9, 543-556 (2008).
[3] Jahn, R. and Scheller, R. H. "SNAREs--engines for membrane fusion". Nat. Rev. Mol. Cell Biol. 7, 631-643 (2006).
[4] Shillcock, J. C. and Lipowsky, R. "Tension-induced fusion of bilayer membranes and vesicles". Nat. Mater. 4, 225-228 (2005).
[5] Schuy, S. and Janshoff, A. "Thermal expansion of microstructured DMPC bilayers quantified by temperature-controlled atomic force microscopy". ChemPhysChem 7, 1207-1210 (2006).
[6] Pan, J. J., Heberle, F. A., Tristram-Nagle, S., Szymanski, M., Koepfinger, M., Katsaras, J. and Kucerka, N. "Molecular structures of fluid phase phosphatidylglycerol bilayers as determined by small angle neutron and X-ray scattering". BBA - Biomembranes 1818, 2135-2148 (2012).
[7] Andersen, T., Kyrsting, A. and Bendix, P. M. "Local and transient permeation events are associated with local melting of giant liposomes". Soft Matter 10, 4268-4274 (2014).
[8] Andersen, T., Bahadori, A., Ott, D., Kyrsting, A., Reihani, S. N. and Bendix, P. M. "Nanoscale phase behavior on flat and curved membranes". Nanotechnology 25, 505101 (2014).
[9] Kyrsting, A., Bendix, P. M., Stamou, D. G. and Oddershede, L. B. "Heat Profiling of Three-Dimensionally Optically Trapped Gold Nanoparticles using Vesicle Cargo Release". Nano Lett. 11, 888-892 (2011).
[10] McDougall, C., Stevenson, D. J., Brown, C. T. A., Gunn-Moore, F. and Dholakia, K. "Targeted optical injection of gold nanoparticles into single mammalian cells". J. Biophotonics 2, 736-743 (2009).
[11] Li, M., Lohmuller, T. and Feldmann, J. "Optical Injection of Gold Nanoparticles into Living Cells". Nano Lett. 15, 770-775 (2015).
[12] Yeheskely-Hayon, D., Minai, L., Golan, L., Dann, E. J. and Yelin, D. "Optically Induced Cell Fusion Using Bispecific Nanoparticles". Small 9, 3771-3777 (2013).
[13] Rørvig-Lund, A., Bahadori, A., Semsey, S., Bendix, P. M. and Oddershede, L. B. "Vesicle Fusion Triggered by Optically Heated Gold Nanoparticles". Nano Lett. 15, 4183-4188 (2015).
[14] Richardson, A. C., Reihani, N. and Oddershede, L. B. "Combing confocal microscopy with precise force-scope optical tweezers". Proceedings of SPIE 6326, 632628 (2006).
[15] Saarikangas, J., Hakanen, J., Mattila, P. K., Grumet, M., Salminen, M. and Lappalainen, P. "ABBA regulates plasma-membrane and actin dynamics to promote radial glia extension". J. Cell Sci. 121, 1444-1454 (2008).
[16] Weinberger, A., Tsai, F.-C., Koenderink, Gijsje H., Schmidt, T. F., Itri, R., Meier, W., Schmatko, T., Schröder, A. and Marques, C. "Gel-Assisted Formation of Giant Unilamellar Vesicles". Biophys. J. 105, 154-164 (2013).
[17] Kreibig, U. and Vollmer, M. *Optical Properties of Metal Clusters*, vol. 25, 1995.
[18] Mie, G. "Beitrage zur Optik Truber Medien, Speziell Kolloidaler Metallosungen". Leipzig, Annalen der Physik 25, 377-445 (1908).

[19] Bendix, P. M., Reihani, S. N. S. and Oddershede, L. B. "Direct Measurements of Heating by Electromagnetically Trapped Gold Nanoparticles on Supported Lipid Bilayers". ACS Nano 4, 2256-2262 (2010).
[20] Richardson, H. H., Hickman, Z. N., Govorov, A. O., Thomas, A. C., Zhang, W. and Kordesch, M. E. "Thermooptical properties of gold nanoparticles embedded in ice: Characterization of heat generation and melting". Nano Lett. 6, 783-788 (2006).
[21] Govorov, A. O. and Richardson, H. H. "Generating heat with metal nanoparticles". Nano Today 2, 30-38 (2007).
[22] Link, S. and El-Sayed, M. A. "Size and Temperature Dependence of the Plasmon Absorption of Colloidal Gold Nanoparticles". J. Phys. Chem. B 103, 4212-4217 (1999).
[23] Qin, Z. and Bischof, J. C. "Thermophysical and biological responses of gold nanoparticle laser heating". Chem. Soc. Rev. 41, 1191-1217 (2012).
[24] Seol, Y., Carpenter, A. E. and Perkins, T. T. "Gold nanoparticles: enhanced optical trapping and sensitivity coupled with significant heating". Opt. Lett. 31, 2429-2431 (2006).
[25] Hansen, P. M., Bhatia, V. K., Harrit, N. and Oddershede, L. "Expanding the optical trapping range of gold nanoparticles". Nano Lett. 5, 1937-1942 (2005).
[26] Svoboda, K. and Block, S. M. "Optical Trapping of Metallic Rayleigh Particles". Opt. Lett. 19, 930-932 (1994).
[27] Baumgart, T., Hunt, G., Farkas, E. R., Webb, W. W. and Feigenson, G. W. "Fluorescence Probe Partitioning Between Lo/Ld Phases in Lipid Membranes". BBA-Biomembranes 1768, 2182-2194 (2007).
[28] Klausner, R. D. and Wolf, D. E. "Selectivity of Fluorescent Lipid Analogs for Lipid Domains". Biochemistry 19, 6199-6203 (1980).
[29] Bendix, P. M. and Oddershede, L. B. "Expanding the Optical Trapping Range of Lipid Vesicles to the Nanoscale". Nano Lett. 11, 5431-5437 (2011).
[30] Peters, R., Peters, J., Tews, K. H. and Bahr, W. "A Microfluorimetric Study of Translational Diffusion in Erythrocyte Membranes". BBA-Biomembranes 367, 282-294 (1974).
[31] Torchilin, V. P. "Recent advances with liposomes as pharmaceutical carriers". Nat. Rev. Drug Discov. 4, 145-160 (2005).
[32] Rawle, R. J., Lengerich, B., Chung, M., Bendix, P. M. and Boxer, S. G. "Vesicle Fusion Observed by Content Transfer across a Tethered Lipid Bilayer". Biophys. J. 101, L37-L39 (2011).
[33] Zhao, H., Pykalainen, A. and Lappalainen, P. "I-BAR domain proteins: linking actin and plasma membrane dynamics". Curr. Opin. Cell Biol. 23, 14-21 (2011).
[34] Saarikangas, J., Zhao, H., Pykalainen, A., Laurinmaki, P., Mattila, P. K., Kinnunen, P. K., Butcher, S. J. and Lappalainen, P. "Molecular mechanisms of membrane deformation by I-BAR domain proteins". Curr. Biol. 19, 95-107 (2009).
[35] Barooji, Y. F., Rørvig-Lund, A., Semsey, S., Reihani, S. N. S. and Bendix, P. M. "Dynamics of membrane nanotubes coated with I-BAR". Sci. Rep. 6, 30054 (2016).
[36] Prevost, C., Zhao, H., Manzi, J., Lemichez, E., Lappalainen, P., Callan-Jones, A. and Bassereau, P. "IRSp53 senses negative membrane curvature and phase separates along membrane tubules". Nat. Commun. 6, 8529 (2015).
[37] Ma, H., Tian, P., Pello, J., Bendix, P. M. and Oddershede, L. B. "Heat generation by irradiated complex composite nanostructures". Nano Lett. 14, 612-619 (2014).
[38] Ma, H., Bendix, P. M. and Oddershede, L. B. "Large-scale orientation dependent heating from a single irradiated gold nanorod". Nano Lett. 12, 3954-3960 (2012).
[39] Baffou, G., Girard, C. and Quidant, R. "Mapping heat origin in plasmonic structures". Phys. Rev. Lett. 104, 136805 (2010).
[40] Aratyn, Y. S., Schaus, T. E., Taylor, E. W. and Borisy, G. G. "Intrinsic dynamic behavior of fascin in filopodia". Mol. Biol. Cell 18, 3928-3940 (2007).
[41] Bendix, P. M., Koenderink, G. H., Cuvelier, D., Dogic, Z., Koeleman, B. N., Brieher, W. M., Field, C. M., Mahadevan, L. and Weitz, D. A. "A quantitative analysis of contractility in active cytoskeletal protein networks". Biophys. J. 94, 3126-3136 (2008).
[42] Tsai, F. C. and Koenderink, G. H. "Shape control of lipid bilayer membranes by confined actin bundles". Soft Matter 11, 8834-8847 (2015).
[43] Kirkham, G. R., Britchford, E., Upton, T., Ware, J., Gibson, G. M., Devaud, Y., Ehrbar, M., Padgett, M., Allen, S., Buttery, L. D. and Shakesheff, K. "Precision Assembly of Complex Cellular Microenvironments using Holographic Optical Tweezers". Sci. Rep. 5, 8577 (2015).
[44] Grier, D. G. "A revolution in optical manipulation". Nature 424, 810-816 (2003).
[45] Dholakia, K., Spalding, G. and MacDonald, M. "Optical tweezers: the next generation". Phys. World 15, 31-35 (2002).